Spectrochimica Acta Part A: Molecular and Biomolecular Spectroscopy 365 (2027) 128783

Contents lists available at ScienceDirect

Spectrochimica Acta Part A:
Molecular and Biomolecular Spectroscopy

journal homepage: www.journals.elsevier.com/spectrochimica-acta-part-a-molecular-and-biomolecular-spectroscopy

Integrated spectroscopic characterization and exploratory Raman-based chemometric analysis of pigments and inks in historical manuscripts and early printed books from the university library of Cagliari

Stefania Porcu *, Giulia Pruna, Lorenzo Minnai, Giancarlo Cappellini, Daniele Chiriu *

Department of Physics, University of Cagliari Cittadella Universitaria, SP no. 8 km 0.700–09042, Monserrato, Italy

HIGHLIGHTS

- Portable Raman, FORS, luminescence and colorimetry were integrated in situ.
- Historical manuscript pigments were identified non-invasively.
- PCA revealed compositional relationships among manuscripts and pigments.
- SIMCA and LDA enabled preliminary provenance and authenticity assessment.
- Integrated spectroscopy and chemometrics support cultural heritage diagnostics.

GRAPHICAL ABSTRACT

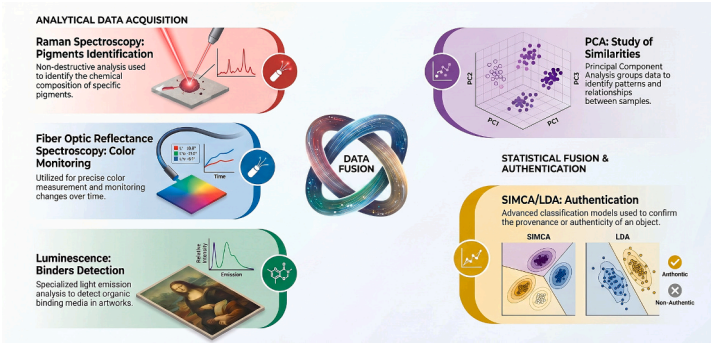

ARTICLE INFO

Keywords:
Cultural heritage
Spectroscopy
Chemometric modeling
Ancient books

ABSTRACT

The identification and characterization of pigments and inks in historical manuscripts and artworks plays a crucial role in understanding artistic techniques, material composition, provenance, and authenticity. In this study, non-invasive in-situ analytical techniques, principal component analysis and supervised chemometric modeling are employed to investigate selected manuscripts dated between the 14th and 18th centuries and preserved at the University Library of Cagliari (BUCA). Micro-Raman spectroscopy provides molecular and structural information on pigment composition and degradation processes, while fiber optic reflectance spectroscopy (FORS) and colorimetric measurements allow the characterization of chromatic properties and their correlation with specific materials. Luminescence spectroscopy was further used to support pigment identification through emission features under UV excitation. Additionally, Principal Component Analysis (PCA) was applied to the Raman datasets to explore patterns and similarities among pigments and inks, whereas FORS, luminescence spectroscopy, and colorimetric measurements provided complementary information for material characterization. Building on this exploratory approach, supervised chemometric models based on Soft Independent Modeling of Class Analogy (SIMCA) and Linear Discriminant Analysis (LDA) were evaluated as a preliminary, proof-of-concept framework for comparing the spectral profiles of pigments and inks across manuscripts, and for illustrating a possible future approach to provenance screening. These methods offer a preliminary framework for distinguishing among the manuscripts examined and for flagging anomalous samples,

* Corresponding authors.
E-mail addresses: stefania.porcu@dsf.unica.it (S. Porcu), daniele.chiriu@unica.it (D. Chiriu).

https://doi.org/10.1016/j.saa.2026.128783
Received 20 June 2026; Received in revised form 7 September 2026; Accepted 11 September 2026
Available online 15 September 2026
1386-1425/© 2026 The Authors. Published by Elsevier B.V. This is an open access article under the CC BY license (http://creativecommons.org/licenses/by/4.0/).

pending validation on a larger, independent dataset. The integration of these techniques within a compact and portable system demonstrates its effectiveness for non-destructive cultural heritage diagnostics. In this work, a preliminary exploratory analysis illustrates the potential for future combination of Raman, FORS, luminescence, and colorimetric information within integrated chemometric workflows, providing a proof-of-concept basis for more extensively validated approaches to authenticity screening and provenance studies. This multi-analytical approach contributes to the development of a systematic methodology for pigment identification and characterization and offers new insights into the historical, artistic, and material context of the manuscripts investigated.

1. Introduction

Cultural heritage represents the collective memory of human societies incorporating both tangible and intangible assets that embody historical, artistic, and social values transmitted across generations. [1–5] Among these, illuminated manuscripts constitute a particularly significant category, as they integrate textual content with highly refined pictorial elements, offering a unique insight into the cultural, technological, and artistic contexts of their production.[6–9] The art of miniature painting has its origins in antiquity, with early examples dating back to the 2nd century. [10,11] However, it increased especially during the medieval and Renaissance periods in Europe and the Middle East, where manuscript illumination became one of the most sophisticated forms of artistic expression. [12–14] These works were not merely decorative; rather, they played a crucial role in visual communication, education, and the transmission of religious and cultural narratives. In many cases, miniatures represent the only surviving evidence of pictorial traditions, as large-scale artworks such as wall paintings or panel paintings have often been lost, deteriorated, or significantly altered over time. [15–18]

The study of pigments and materials used in these manuscripts can therefore provide valuable information about artistic practices, workshop organization, and even cultural exchanges between different geographical regions. Despite their importance, manuscripts are highly vulnerable to degradation processes. Environmental factors such as light exposure, humidity, temperature fluctuations, and atmospheric pollutants can lead to chemical and physical alterations of pigments and supports. Additionally, aging and past restoration interventions may further complicate the interpretation of the original materials. For these reasons, the development of reliable, non-invasive analytical methodologies is essential for both the study and conservation of such artifacts. [19–24]

In recent decades, the field of cultural heritage science has increasingly relied on analytical techniques based on light–matter interaction, which allow researchers to investigate the composition and properties of materials without sampling or damaging the objects. Among these, micro-Raman spectroscopy, Fiber Optic Reflectance Spectroscopy and Luminescence spectroscopy have emerged as powerful and complementary tools for pigment characterization. [24,25]

Micro-Raman spectroscopy is widely recognized for its ability to provide detailed information on the molecular structure and crystalline phases of materials through the analysis of vibrational modes. This technique allows the identification of both inorganic and organic pigments, as well as degradation products, making it particularly suitable for the study of historical artifacts. Furthermore, Raman spectroscopy can sometimes offer insights into the chronological aspects of materials, contributing to dating and authentication studies. [26–30]

In addition, Fiber Optic Reflectance Spectroscopy operates by measuring the fraction of incident radiation reflected by a surface over a broad spectral range, typically from the visible to the near infrared. The resulting spectra are directly related to the optical properties and color of the material, allowing for the identification of pigments based on their characteristic reflectance features. This technique is particularly helpful for analyzing large areas and for correlating spectral data with visual perception. [31–34]

Similarly, Luminescence spectroscopy provides additional information by detecting the emission of light from a material following excitation, typically in the ultraviolet region. Many pigments and binders exhibit characteristic luminescence responses, which can serve as diagnostic markers for their identification. [35]

Alongside spectroscopic techniques, colorimetric analysis plays an important role in the study of artworks and manuscripts. [22]

By correlating colorimetric data with spectroscopic results, it is possible to establish a direct relationship between observed colors and specific pigments or mixtures. This approach is particularly useful for verifying the consistency between visual appearance and material composition, as well as for detecting alterations, retouching, or degradation phenomena that may affect the original chromatic balance.

While individual spectroscopic measurements provide valuable information on specific points, the analysis of large datasets requires advanced statistical methods to extract meaningful patterns. Principal Component Analysis is a multivariate statistical technique widely used to reduce data dimensionality while preserving the most significant sources of variance.

Applied to Raman spectral datasets, the Principal Component Analysis allows the identification of similarities and differences between samples by projecting the data into a lower-dimensional space defined by principal components. This approach facilitates the classification of pigments, the detection of clusters corresponding to specific materials or techniques, and the identification of outliers. [36–38]

Moreover, PCA can be used to compare unknown samples with reference spectra stored in databases, supporting attribution studies and the investigation of stylistic influences.

While PCA is particularly effective as an exploratory tool for identifying spectral similarities and grouping samples according to their compositional features, recent developments in cultural heritage science increasingly rely on supervised chemometric approaches for classification and authentication purposes. Methods such as Soft Independent Modeling of Class Analogy (SIMCA) and Linear Discriminant Analysis (LDA) enable the construction of predictive models capable of assigning unknown samples to predefined classes and evaluating their compatibility with specific historical or geographical groups. By integrating spectroscopic and colorimetric information within a multivariate framework, these approaches offer new opportunities for provenance studies, authenticity assessment, and the detection of anomalous or potentially restored materials. [39] In this work, exploratory PCA and supervised chemometric modeling are jointly employed to investigate the classification potential of the analyzed manuscripts.

It should be stated from the outset that the present study does not establish or validate a predictive classifier that can be directly used for manuscript provenance determination. Rather, the study compares the spectral characteristics of pigments and inks of the same color across the seven manuscripts examined; focuses subsequently on the black and yellow materials, which show relatively pronounced differences in the current dataset and illustrates, as a proof of concept, how these material characteristics might be used in future studies to evaluate the compatibility of an unknown manuscript with established historical reference groups. Three distinct tasks are addressed throughout this work: pigment/ink identification (Section 3.3), exploratory comparison among the investigated manuscripts (Section 3.4), and an illustrative

demonstration relevant to future provenance screening of unknown manuscripts (Section 3.5).

By revealing unknown correlations within the data, this method provides a powerful tool for exploring the relationships between materials, artistic practices, and historical contexts.

The present work focuses on a selection of manuscripts preserved at the Biblioteca Universitaria di Cagliari (BUCA), dating from the 14th to the 18th century. These artifacts were selected for their artistic value, state of preservation, and the presence of richly colored miniatures. In this context, the analyses were carried out using a set of portable instrumentation, specifically employed in this study to enable in-situ, non-invasive investigations directly within the library environment. This approach minimizes the risks associated with the transportation and handling of fragile objects, while ensuring the acquisition of reliable analytical data.

The integration of multiple techniques within the same portable system further enhances the strength of the analysis, allowing for cross-validation of independent datasets and improving the accuracy of pigment identification. By combining complementary analytical methods with advanced data processing, this research aims to establish a methodological framework for the study of historical pigments. The results contribute not only to the scientific understanding of the materials and techniques used in the manuscripts but also to the broader goals of cultural heritage preservation, authentication, and valorization.

2. Materials and methods

2.1. Samples

In Fig. 1 the images relative to the above target samples are reported.

- *Biblicae Historiae: Magno artificio depictae, et utilitatis publicae causa latinis Epigrammatibus a Georgio Aemylio illustratae*, printed in 1539 and enriched with woodcuts by Hans Sebald Beham, which were



Fig. 1. (a) Biblicae Historiae: Magno artificio depictae, et utilitatis publicae causa latinis Epigrammatibus a Georgio Aemylio illustratae. (b) Joannes de Lignano in Clementinas by Giovanni da Legnano and Adiciones Johan-nis Calderini super Clementinis by Giovanni Calderini. (c and d) Tratado de algunas sciencias matematicas by Salvatore Pala. (e) "Opus de intellectu et causis mirabilium effectuum"; (f) "Explicit Biblia"; (g) "Compendium Theologicae Veritatis.

colored by hand around the end of the eighteenth century by local painters commissioned by the owner Giola (Fig. 1a).

- *Joannes de Lignano in Clementinas* by Giovanni da Legnano and *Adiciones Johannis Calderini super Clementinis* by Giovanni Calderini, two texts bound together by an anonymous bookbinder in the 19th century. Both authors belong to the Bolognese school. The first text dates back to 1378, while the second was written between 1350 and 1378, and they consist of a collection of decretals of Pope Clement *V* (Fig. 1b).
- *Tratado de algunas sciencias matematicas* by Salvatore Pala, a mathematics treatise in Castilian published in 1628. The work is part of a three-book manual for educational use (Fig. 1c and d).
- *The "Opus de intellectu et causis mirabilium effectuum"* published in Florence at the beginning of the sixteenth century by the philosopher and doctor Andrea Cattaneo (Fig. 1e).
- *A Bible* printed in Venice in 1476 from Editors Franz Renner and Niccolò da Francoforte (Fig. 1f).
- *A Theology manuscript* by (saint) Albertus Magnus "Compendium Theologicae Veritatis" (probably) of the beginning of the fifteenth century (Fig. 1g) (See Table 1).

2.2. Experimental techniques

To analyze the primary pigments found in the samples, including black, red, yellow, green, and blue, a series of advanced spectroscopic and reflectance measurements were conducted.

Near infrared micro-Raman scattering measurements were carried out in back scattering geometry with the 1064 nm line of an Nd:YAG laser. Measurements were performed with a compact spectrometer B&WTEK (Newark-USA) i-Raman Ex integrated system with a spectral resolution of 8 cm^{-1}. All the spectra were collected in 60 s (five replicas) and power excitation between 5 and 10 mW concentrated in a spot of 0.3 mm^2 on the surface through a Raman Video Micro Sampling System BAC151B equipped with a 20× Olympus objective to select the area on the samples. For each measurement point, the five Raman replicates and three FORS replicates were averaged prior to any statistical treatment, and the averaged spectrum was used as the single input observation for PCA, SIMCA, and LDA; consequently, in all reported analyses n refers to the number of independent measurement points (one per sampled area per manuscript), not to the number of individual replicate spectra or to the number of manuscripts.

Reflectance measurements were performed by means of a Laser driven Xenon lamp (EQ-99×) with wide emission spectrum from 200 to 2000 nm and average optical power of 1 mW/nm. The source was coupled with an optical fiber to an integrating sphere and to an Advantes Sensiline Avaspec-ULS-TEC Spectrometer (spectral range 250–900 nm). The measurements were taken in 10° reflection mode (including the specular component), using a $BaSO_4$ plate as a reference. Each measurement for every sample and time interval was conducted three times. The results obtained from the reflectance measurements were related to the D65 illuminant and the CIE 1931 2° standard colorimetric observer. The CIE coordinates were obtained by using the ColorConvert v7.77 software. Reflectance spectra were integrated over the wavelength range 380–780 nm to compute the tristimulus XYZ values under the CIE 1931 2° standard observer and D65 illuminant, prior to conversion into Lab* coordinates. The change of color was characterized according to the change in lightness ΔL, red–green difference Δa, yellow–blue difference Δb, and total calculation of color difference ΔE using the following formula:

$$\Delta E = \sqrt{(\Delta L)^2 + (\Delta a)^2 + (\Delta b)^2} \quad (1)$$

Luminescence measurements were performed by means of a 365 nm LED. The source was coupled with an optical fiber to an integrating sphere and to an Advantes Sensiline Avaspec-ULS-TEC Spectrometer (spectral range 250–900 nm). In all acquisitions, a 470 nm long-pass filter was used to suppress the intrinsic emission of the support.

2.3. Data hierarchy

Averaging the technical replicates is appropriate. However, multiple spatial measurement points from the same manuscript remain nested within the same historical object and cannot be treated as equivalent to multiple independent manuscripts; in the present dataset, one point per color per manuscript was acquired, so the independent-manuscript count and the independent-measurement-point count coincide for each color, but this should not be assumed to hold in future studies with denser spatial sampling.

3. Results and discussion

3.1. Reflectance and colorimetry

The discussion of the results begins with the reflectivity measurements, as they provide direct insight into the optical properties of the investigated areas and a first indication of the characteristics of the pigments. Representative spectra acquired from selected colored regions are shown in Fig. 2 and S1-S6 in Supporting information, illustrating the main trends observed across the analyzed manuscripts. Overall, the spectra display a high degree of consistency, pointing to a relatively homogeneous palette among the different works.

Across all samples, the spectral behavior varies systematically with

Table 1
Data hierarchy.

Manuscript	Production/ printing date	Illumination date (if different)	Documented historical provenance	Support	Independent spatial points / color	Raman & FORS technical replicates / point
Biblicae Historiae	1539 (print)	c. late 18th c. (hand coloring)	Owned/commissioned by Giola	Paper	1 / color (red, black, blue, green, yellow)	5 Raman +3 FORS
Joannes de Lignano in Clementinas	1378	–	Bolognese school	Parchment	1 / color	5 Raman +3 FORS
Adiciones Johannis Calderini super Clementinis	1350–1378	–	Bolognese school	Parchment	1 / color	5 Raman +3 FORS
Tratado de algunas sciencias matematicas	1628	–	Salvatore Pala, Castilian, educational manual	Paper (cellulose)	1 / color	5 Raman +3 FORS
Opus de intellectu et causis mirabilium effectuum	early 16th c.	–	Andrea Cattaneo, Florence	Parchment	1 / color (red, blue; green/ pink not usable, see §3.3)	5 Raman +3 FORS
Explicit Biblia	1476	–	Franz Renner & Niccolò da Francoforte, Venice	Paper (cellulose)	1 / color (red, blue)	5 Raman +3 FORS
Compendium Theologicae Veritatis	probably early 15th c.	–	Attributed to (saint) Albertus Magnus	Parchment	1 / color	5 Raman +3 FORS

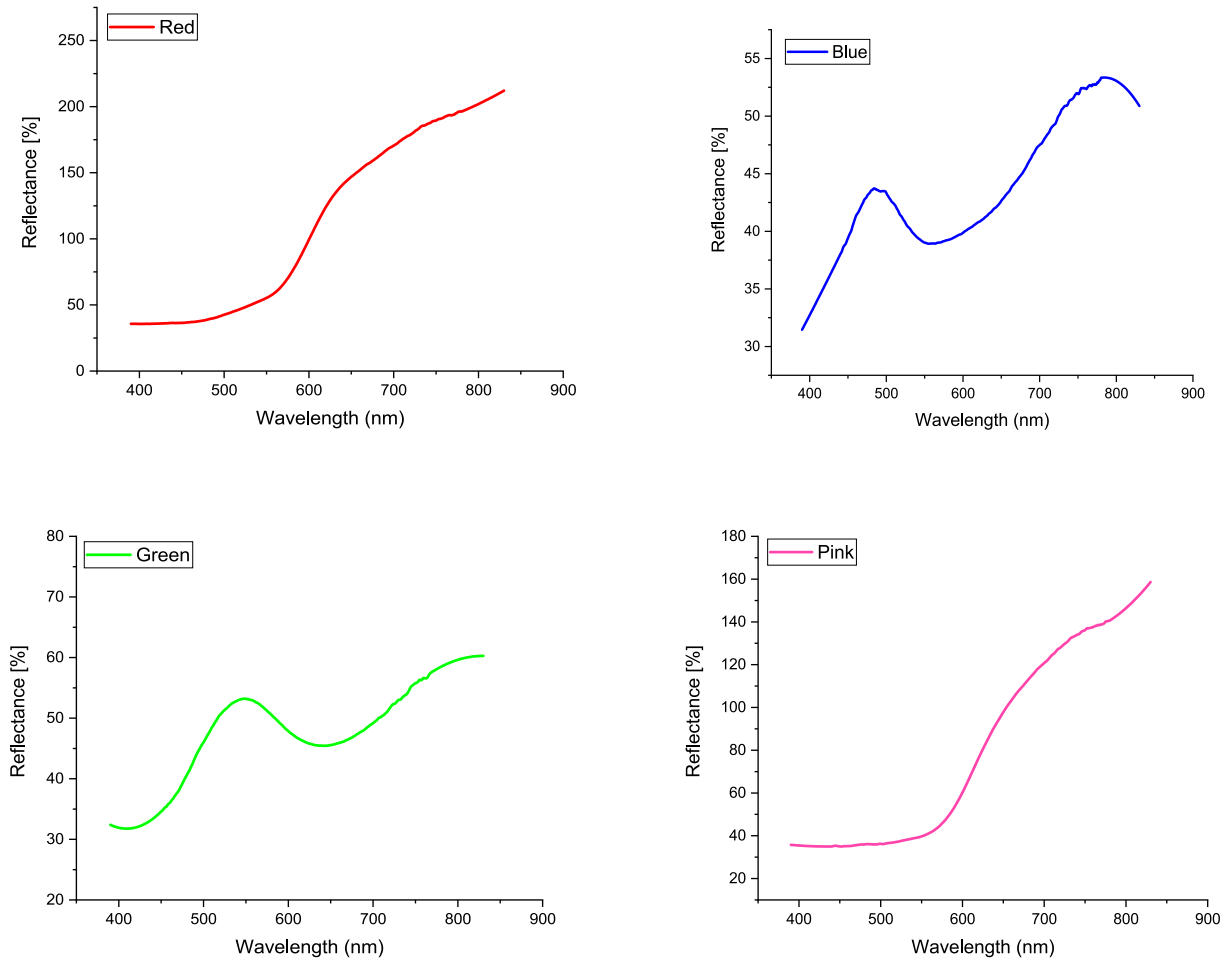

Fig. 2. Reflectance spectra of colors analyzed in "Opus de intellectu et causis mirabilium effectuum".

color, revealing well-defined and reproducible features. Red areas are characterized by a pronounced increase in reflectance beyond approximately 600 nm, resulting in a steep spectral slope at longer wavelengths. The reflectance spectrum of the pink region follows the same spectral profile as the red pigment, indicating similar absorption features, although with a generally reduced reflectance across the investigated spectral range. This behavior suggests a dilution or mixing of the red pigment with a white component, leading to a decrease in reflectance intensity while preserving the overall spectral shape. Blue regions, in contrast, exhibit a distinct reflectance maximum in the 450–500 nm range, followed by a progressive decrease toward higher wavelengths. Green areas show broader and more gradual maxima between 500 and 570 nm, reflecting a more complex spectral profile. Yellow regions are distinguished by a smoother and more continuous increase in reflectance between 560 and 590 nm, without sharp features but with a clearly identifiable trend. Black inks, on the other hand, display uniformly low reflectance values across the entire spectral range, with minimal variation, consistent with their strong light-absorbing behavior.

A recurring feature in many spectra is the presence of a luminescent background, particularly noticeable at longer wavelengths. In some cases, reflectance values exceed 100%, indicating a contribution from luminescence rather than pure reflection. This effect suggests the presence of emissive components within the pictorial layer, which generate an additional signal in the red to near-infrared region, superimposed on the reflectance response.

Starting from the reflectance spectra, the CIE Lab coordinates were calculated and reported in Table 2. Variations in the Lab* coordinates across samples are consistent with, but do not by themselves demonstrate, differences in pigment mixture (e.g., malachite vs. azurite, or orpiment vs. goethite) or in support material (parchment vs. cellulose

Table 2
CIE Lab coordinates.

	L	a	b		L	a	b
Biblicae Historiae				Clementinas (Giovanni da Legnano)			
red	58.0	17.0	16.7	red	59.5	42.9	34.2
black	49.1	0.6	6.5	blue	42.6	−3.3	−19.6
blue	44.1	−12.3	−6.8	green	59.4	−11.8	15.4
green	69.8	−11.7	30.2	yellow	81.9	3.5	48.6
yellow	84.1	1.8	53.8	black	66.2	2.6	23.6
Clementinas (Giovanni Calderini)				Tratado de algunas sciencias matematicas			
red	60.5	43.9	25.9	red	62.3	41.5	25.4
green	68.0	−12.8	14.4	black	57.2	2.0	14.9
blue	35.6	−1.0	−22.4	green	57.4	−21.1	20.4
yellow	saturation due to gold			blue	34.4	1.9	−20.2
black	32.6	1.0	−2.9	yellow*	91.2	3.9	26.8
Opus de intellectu et causis mirabilium effectuum				Explicit Biblia			
red*	86.3	31.0	33.1	red	47.4	17.4	−2.2
blue	69.6	−1.4	1.5	blue	46.8	1.2	−8.9
green	75.7	−8.7	16.8				
pink*	74.4	22.4	15.0				
Compendium theologiae veritatis							
blue*	46.8	1.2	−9.0				
green	80.9	−8.5	12.4				
pink*	80.2	27.1	9.2				

* Apparent reflectance >100% (luminescence-affected).

combined with calcium hydroxide); such compositional attributions rely primarily on the Raman evidence discussed in Section 3.3, rather than on the colorimetric data alone. Color differences noted between samples in this discussion are described qualitatively on the basis of the Lab* coordinates reported in Table 2.

Among the entries in Table 2, the Lab* coordinates for: red and pink pigments of Opus de intellectu et causis mirabilium effectuum, blue and pink pigments of Compendium Theologicae Veritatis and yellow pigmeny of Tratado de Matematicas were derived from reflectance spectra showing apparent reflectance above 100% in the red/near-infrared region, indicating a luminescence contribution superimposed on the reflectance signal. These coordinates were retained uncorrected and flagged as approximate (*), consistent with the proposed future data-fusion strategy described in Section 3.6, in which colorimetric coordinates would be bypassed for luminescent pigments/areas.

3.2. Luminescence analysis

To further investigate the regions in which reflectance spectra suggested the presence of a luminescent background, complementary luminescence measurements were performed. In all acquisitions, a 470 nm long-pass filter was used to suppress the intrinsic emission of the support, typically occurring in the 430–460 nm range and attributable to parchment or paper. This precaution allowed a more reliable detection of the emission features associated with the pictorial layer. The recorded spectra were subsequently deconvoluted in order to separate the individual contributions arising from the support and from the pigment–binder system, thus enabling a clearer interpretation of the observed signals. The deconvolution was performed after baseline subtraction using Gaussian peak functions, with two components fitted simultaneously. The emission band at 630–660 nm was observed at a consistent spectral position across pigments of different colors, which points to a common organic component rather than a color-specific inorganic pigment. Organic red lake dyestuffs such as madder (alizarin/purpurin-based), commonly employed in illuminated manuscripts, are reported in the literature to display luminescence emission in a comparable 600–650 nm range under UV/visible excitation [40,41], alongside organic binders and support-related degradation products, as possible sources of this signal.

Representative spectra obtained for "*Opus de intellectu et causis mirabilium effectuum*" (Fig. 3) exhibit emission bands consistently located within the 630–655 nm range, regardless of the color of the analyzed areas. The stability of both the spectral position and the overall profile strongly suggests that the luminescence originates predominantly from the binder rather than from the pigments themselves. This interpretation is supported by the fact that many organic binding media commonly

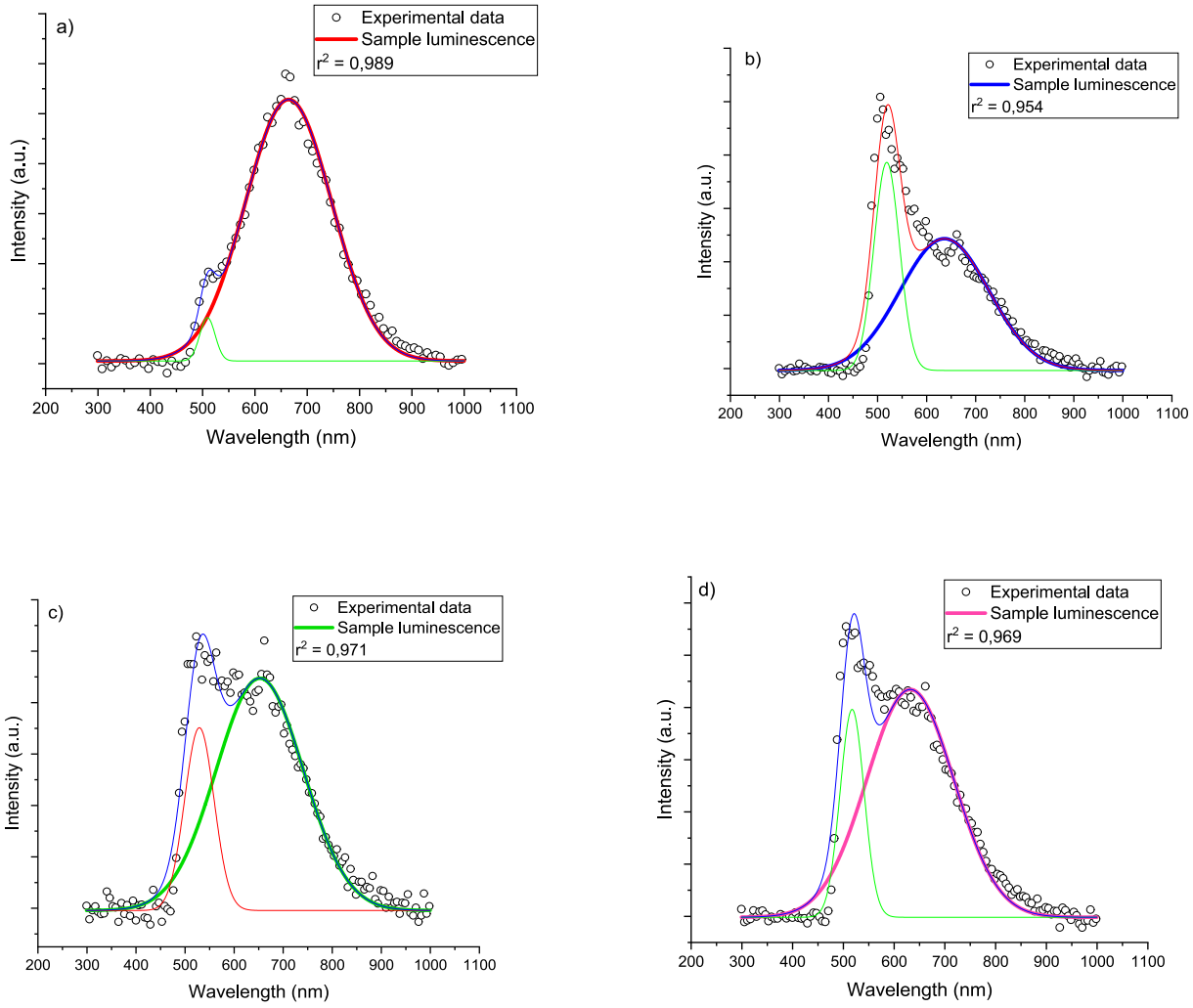

Fig. 3. Luminescence spectra of selected inks from "Opus de intellectu et causis mirabilium effectuum". Representative spectra of Red Ink (A), Blue Ink (B), Green Ink (C), and Pink Ink (D) are shown. The spectra were deconvoluted to separate contributions from the support, shown with a thinner line, and from the pigment, indicated with a thicker line in the corresponding pigment color. (For interpretation of the references to color in this figure legend, the reader is referred to the web version of this article.)

employed in historical manuscripts are known to display emission in the red to near-infrared region when excited in the near-ultraviolet (365 nm). In this context, interactions between the binder and the pigment particles may induce slight modifications in the local electronic environment, potentially affecting both absorption and emission processes, although without significantly altering the overall spectral signature.

A comparable behavior is observed in the *Explicit Biblia* (Fig. S7), where emission maxima are centered around 660 nm across all investigated regions. The uniformity of these features further supports the hypothesis of a binder-dominated luminescent response, consistent with the widespread use of organic materials in manuscript production. These substances, often derived from natural sources, are known to contribute significantly to the optical response of the pictorial layer, especially when excited under the experimental conditions adopted in this study.

Similarly, in the *Compendium Theologicae Veritatis* manuscript (Fig. S8), the detected emission bands fall within a slightly broader interval, between 645 and 660 nm, effectively bridging the ranges observed in the other analyzed codices. The recurrence of emission features within this narrow spectral window across different manuscripts, time periods, and color areas reinforces the interpretation that the luminescence is largely governed by the binder component. Minor variations in peak position and intensity can reasonably be attributed to differences in binder composition, aging processes, or specific interactions with the associated pigments. Nevertheless, the overall coherence of the spectral response points to a common underlying mechanism, highlighting a characteristic optical behavior of historical manuscript materials.

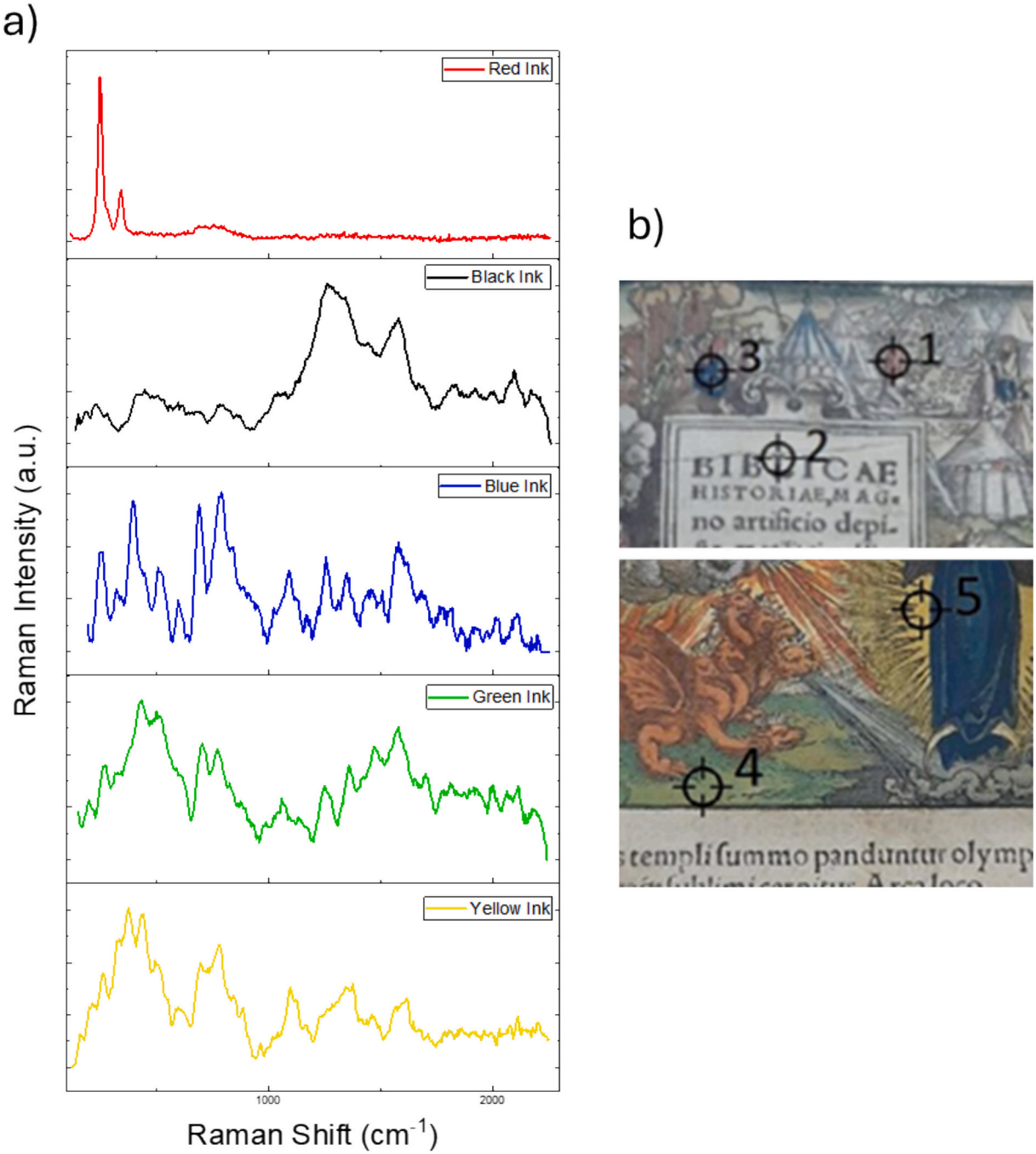

Fig. 4. Raman spectra collected for "Biblicae Historiae" (a) in the points evidenced in figure b.

3.3. Raman analysis

Fig. 4a reports the Raman spectra collected for "Biblicae Historiae" in the points evidenced in Fig. 4b. Starting from point 1 (red), the main Raman vibrational modes are centered at 251, 286 and 343 cm^{-1} ascribable to red cinnabar. Other two weak broad bands at 700 and 790 cm^{-1} are associated to calcium hydroxide, tentatively attributed to a deacidification treatment. Point 2 (black) presents two bands at 1270 and 1584 cm^{-1} compatible with carbon black pigment. Point 3 is associated with a blue pigment constituted by a mixture of azurite (256, 335, 398, 840, 1092, 1458 and 1581 cm^{-1}) and malachite (444, 512, 1090 cm^{-1}). Other bands in the spectrum are associated to calcium hydroxide and cellulose from the paper. The green pigment of point 4 is associated principally to malachite and traces of azurite. Point 5 presents a yellow pigment with a mix of orpiment (160, 299, 350 cm^{-1}), goethite (300, 377, 480 and 550 cm^{-1}) and traces of malachite. Cellulose-related bands (965, 1099, 1122 cm^{-1}) confirm paper as the support, distinguishing it from the earlier parchment-based codices.

The Raman spectra and the analyzed points of the other manuscripts are reported in the supporting informations file (S9–S13).

S9 reports the Raman spectra collected for "Clementinas" in the points of S9c. Starting from point 1 of Fig. 3a and b, the main Raman vibrational modes correspond to red cinnabar. The blue pigments of point 2 of S9a and point 3 of S9b are constituted by azurite with traces of malachite and lazurite (257, 534 and 770 cm^{-1}). In the spectrum it is also evident the contribution of the parchment (1024, 1082, 1258, 1341 and 1450 cm^{-1}). The green pigments of point 3 (S9a) and point 2 (S9b) are associated to malachite with traces of azurite. The Raman vibrational modes of gold yellow pigments of points 4 S9a and point 4 of S9b show bands tentatively assigned to a gold-containing binder compound (242, 456 and 504 cm^{-1}). The black pigments are associated with carbon black.

Also in the case of "*Tratado de algunas sciencias matematicas*", the red pigments are associated to red cinnabar, green pigment to malachite, blue pigments to azurite, while the black pigments are constituted by iron gall ink (248, 397, 554, 1334, 1475 and 1586 cm^{-1}), and yellow pigments by a mixture of lepidocrocite (255, 351, 380 and 528 cm^{-1}) and goethite. Even for this sample it is fundamental the contribution of calcium hydroxide and cellulose in the spectra (S10a and b).

Fig. S11b shows an illustration of the sample "Opus de intellectu et causis mirabilium effectuum" and the representative points where Raman spectra have been collected. In this manuscript, Raman analysis confirmed cinnabar in the red ink (249, 343 cm^{-1}) and azurite in the blue (250, 330, 407 cm^{-1}). Bands from the parchment support (508, 699, 810, 1255, 1647 cm^{-1}) are visible, further confirming the nature of the substrate (S11a). To avoid damage to the green and pink areas the applied laser power was reduced, preventing the acquisition of spectra with sufficient signal-to-noise ratio for reliable pigment identification.

Further, S12a. shows the Raman spectra of the sample "Explicit Biblia" (impressa Venetijs: per Franciscum de halibrun et Nicolaum de frankfordia socios, 1476) in the points reported in Fig. S12b. The spectral data collected from this incunabulum revealed azurite in the blue decorations (249, 403, 1093, 1581 cm^{-1}), while the red ink displayed a mixture of cinnabar (256, 337 cm^{-1}) and purpurin (954, 1138, 1168, 1311 cm^{-1}). The support, unlike previous samples, is paper-based; this is confirmed by cellulose-related peaks (377, 429, 1104 cm^{-1}), in agreement with the manufacturing context.

Finally, Fig. S13. shows the Raman spectra of the sample "Compendium Theologicae Veritatis" (probably) of the beginning of the fifteenth century. Cinnabar remains the dominant red pigment in this manuscript, with peaks at 249 and 344 cm^{-1}. The blue ink is defined by azurite (330, 397, 547 cm^{-1}) with associated calcium hydroxide bands (692, 767 cm^{-1}). The green ink spectrum is partially obscured by noise but presents features assignable to malachite (250, 430, 504, 1260 cm^{-1}). The pink ink reveals both azurite and purpurin, indicating a layered or mixed application of mineral and organic components. The yellow ink area is particularly noteworthy, showing peaks at 311 and 442 cm^{-1} compatible with orpiment, yet slightly shifted; while this could suggest doping with antimony- or arsenic-based impurities, instrumental resolution, band overlap, or crystallinity effects cannot be excluded. Calcium hydroxide is again present (705, 782 cm^{-1}). In gold-decorated regions, no Raman signals from gold are observed, but unidentified binder-related bands are detected. Table 3 summarizes all the results obtained for each sample.

3.4. Principal component analysis (PCA)

Once the Raman spectra, presented in the previous chapter, has been obtained, Principal Component Analysis (PCA) can be performed. PCA is a multivariate analysis technique whose aim is to reduce the dimensionality of the problem by smoothing any spectrum taken of a given color to a linear combination of single spectra, which represents a basis of the space that collects all Raman spectra of the chosen color. To perform this, all spectra of the same color in all works must have the same Raman shift interval and smoothing of these must be performed for the same number of points. On the intensity of the spectra, the same normalization procedure of the given must be carried out, which is a necessary condition to obtain a reliable PCA analysis. The output of the function consists, for each color, of two loading vectors, expressed on the same Raman-shift axis as the input spectra and referred to as the 'principal components', together with two coefficients (scores) per Raman spectrum, representing the coefficients to be applied to the principal components to reconstruct the corresponding spectrum, and a summary graph that allows the two coefficients for each spectrum to be visually represented, allowing to see which spectra are similar, i.e. have a similar composition, and which do not. Rather than isolated spectra of pure compounds, each principal component is a mathematical construct that predominantly reflects, or is associated with, the spectral features shared by several samples of that color. This exploratory PCA is based on the Raman spectra alone, for each color separately; no reflectance or luminescence data are combined with the Raman spectra at this stage. Data fusion with FORS reflectance and luminescence data is not implemented in the SIMCA/LDA demonstration presented in Section 3.5 (which likewise uses Raman PCA scores alone); it is instead proposed as a direction for future work in Section 3.6. Prior to PCA, each Raman spectrum was baseline-corrected, interpolated onto a common wavenumber axis, and mean-centered; the first two principal components accounted, respectively, for 84.81% and 14.14% of the total variance for red (cumulative 98.95%), 51.20% and 22.11% for green (cumulative 73.31%), 82.81% and 13.07% for black (cumulative 95.88%), 40.72% and 28.37% for yellow (cumulative 69.09%), and 45.73% and 22.24% for blue (cumulative 67.97%).

To facilitate the interpretation of the following graphs, each sample was assigned a symbol, as indicated in Table 4.

The results obtained from the PCA analysis of the spectra associated with red pigments are presented in Fig. 5 and the coefficients obtained for the samples are presented in Table 5.

The first principal component is associated with cinnabar and the second principal component with purpurin and calcium hydroxide. In Fig. 6 is evident that the sample "Explicit Biblia" is separated from the rest by positioning itself in the first quadrant, having a high coefficient of the second principal component number. This implies that for this sample content of purpurin and calcium hydroxide, mixed in the pigment or as a treatment of the support, is in significantly greater quantity. From the graph we can also see that the other samples are close to each other and thus have a similar composition.

The same analysis has been performed for all the inks studied.

In the case of blue inks, it was not possible to make a clear division. In Fig. S14, the first principal component picks up some maxima of azurite, lazurite and calcium hydroxide in the first section while in the second it picks up the organic maxima of parchment and cellulose; the second principal component picks up some maxima of the supports and lazurite.

Table 3
Summary of all the components on the analyzed inks throughout the different manuscripts.

Sample		Writing support			Pigment/Ink							
		Cel.	Par	Ca(OH)	Cin.	Az.	Mal.	Pur.	Orp.	C. B.	IGall.	Lep.	Goe
Opus de intellectu et causis mirabilium effectuum	Red		X		Δ	□		○					
	Blue		X										
	Green		X										
	Pink		X										
Explicit Biblia	Red	●●			Δ	□							
	Blue												
Compendium Theologicae Veritatis	Blue		X	+	Δ	□	◊	○	✦				
	Green		X										
	Pink		X	+									
	Red		X										
	Yellow		X	+									
	Gold		X										
Biblicae Historiae	Red	●●●		+	Δ	□	◊		✦	▲			■
	Black												
	Blue												
	Green			+									
	Yellow												
				+									
Clementine by Giovanni da Legnano	Red				Δ	□	◊			▲			
	Blue		X	+									
	Green		X	+									
	Gold			+									
	Black		X	+									
Clementine by Giovanni Calderini	Red				Δ	□	◊			▲			
	Green		X	+									
	Blue			+									
	Gold		X										
	Black												
Tratado	Red	●			Δ	□	◊				◆	✩	■
de Matematicas	Black	●		+									
	Green												
	Blue												
	Yellow												

(●) Cell. = Cellulose; (**X**) Par. = Parchment; (+) CaOH = Calcium Hydroxide; (▲) Cin. = Cinnabar; (□) Az. = Azurite; (◊) Mal = Malachite; (○) Pur. = Purpurin; (✦) Orp. = Orpiment; (▲) C.B. = Carbon Black; (✩) Lep = Lepidocrocite; (■) Goe = Goethite.

Table 4
Symbols used to represent the samples analyzed.

Opus de intellectu et causis mirabilium effectuum	ΔΔ
Explicit Biblia	○
Compendium Theologicae Veritatis	□
Biblicae Historiae	◊
Clementine by Giovanni da Legnano	✦
Clementine by Giovanni Calderini	▲
Tratado de Matematicas	✩

Given the bandwidth of the background found, it is likely that component number two associates some amorphous binding compound that characterizes the pigments. In this case, as we can see in Fig. S15, the aggregation process of the given overlaps "Tratado de Matematicas" and "Clementine" by Giovanni Calderini, separating the other samples, which are positioned on different quadrants. The coefficients obtained for the samples, illustrated in Fig. S15, are presented in Table S1.

The results obtained from the PCA analysis of the spectra associated with green pigments are presented in Fig. S16 while the multiplication coefficients in fig. S17 and Table S2.

In this case, it was observed that the first principal component picks up some of the first peaks of malachite and azurite, with a portion of the final peaks from the support. The second principal component also includes peaks associated with malachite but, in addition, incorporates other peaks from the support and a considerable amount of what appears to be noise, particularly in the second half of the graph. It was also observed that in "Tratado de Matematicas" and "Compendium Theologicae Veritatis", the noisiest datasets, appear to be isolated from the other three.

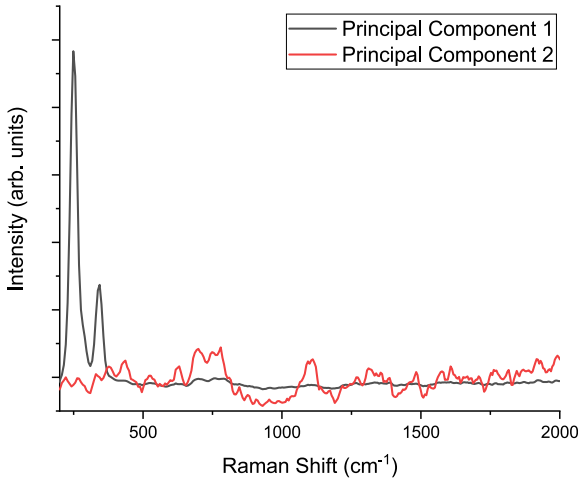

Fig. 5. PCA of red pigments. Raman spectra of the two principal components obtained from PCA on red pigments. (For interpretation of the references to color in this figure legend, the reader is referred to the web version of this article.)

The results obtained from the PCA analysis of the spectra associated with black pigments are presented in Fig. S18, the multiplication coefficients to be used to obtain the black Raman spectra of the respective samples in fig. S19 and the coefficients obtained for the samples in table S3.

The first principal component can be associated with carbon black

Table 5
Coefficients for principal components of red pigments. Values of the coefficients associated with the principal components used to reconstruct the original spectrum of the red pigments.

Sample	PCA 1	PCA 2
Opus de intellectu et causis mirabilium effectuum	0,40,838	0,00934
Explicit Biblia	0,05607	0,99,552
Compendium Theologicae Veritatis	0,40,782	0,0154
Biblicae Historiae	0,40,206	−0,00422
Clementine by Giovanni da Legnano	0,40,907	−0,0455
Clementine by Giovanni Calderini	0,40,924	−0,04338
Tratado de Matematicas	0,40,902	−0,0681

and cellulose, while the second principal component corresponds to iron gall ink and the support. The data aggregation process clearly separates the sample "Tratado de Matematicas" from the others, which are all located in the second quadrant. This suggests that the "Tratado de Matematicas" sample contains a higher amount of iron gall ink in its black pigment.

For yellow inks, PCA clearly separates the two datasets obtained from the "Clementinas" from the rest (Fig. S20). Specifically, the first principal component captures the main peaks of the gold binder and part of the parchment spectrum, while the second principal component appears to be a combination of limonite peaks and peaks from cellulose (S21, Table S4). The "Tratado de Matematicas", which consists of cellulose with a small amount of pigment, is compressed along the vertical axis, supporting this observation. The black and yellow datasets were selected for this proof-of-concept demonstration because visual inspection of the exploratory PCA results presented above indicated comparatively larger inter-manuscript separation for these two colors than for red, blue, and green (compare Figs. 5–6 and S14–S20). This is an exploratory, data-driven choice rather than a pre-specified one. Because the same dataset was used both to select the colors showing the largest separation and to illustrate the classification approach in Section 3.5, the results presented there cannot be regarded as an independent validation of classification performance, nor can they be used to estimate the accuracy expected for unknown manuscripts; they are intended primarily to generate hypotheses for future, independently designed studies. The comparatively weaker separation observed for red, blue, and green pigments does not imply that these materials carry no provenance-relevant information; it may simply reflect the limited number of manuscripts currently available, the specific manuscripts selected, or the applied preprocessing.

3.5. Chemometric modeling for provenance and classification

As stated in the Introduction, the present study does not aim to establish a validated predictive classifier for manuscript provenance. In this section, we explore, as a preliminary proof of concept, the feasibility of applying supervised pattern-recognition methods (SIMCA, LDA) to assess the compatibility of a query sample with a reference group defined from the exploratory PCA of Section 3.4. Specifically, a preliminary workflow leveraging Soft Independent Modeling of Class Analogy (SIMCA) and Linear Discriminant Analysis (LDA) based on the multidimensional spectroscopic trajectories established in the preceding sections, was developed.

The core of this exploratory framework relies on establishing indicative coordinates for each manuscript "class" within a reduced hyperspace. While the exploratory PCA successfully clusters individual books based on their specific ink or pigment formulations (e.g., separating the 14th-century Bolognese legal texts from the 18th-century Spanish mathematical treatise), it lacks a probabilistic assignment criterion. To overcome this, we explore, as a proof of concept, a mathematical criterion for each known historical source using Hotelling's T^2 confidence ellipses, subject to the important statistical warnings set out below.

Mathematically, for a given cluster in the score space defined by the principal components (PC1 and PC2), the distance of any sample vector $\mathbf{x}$ from the class centroid $\boldsymbol{\mu}$ is governed by the Mahalanobis distance (D_M), which accounts for the covariance matrix $\boldsymbol{\Sigma}$ of the class:

$$D_M = \sqrt{(\mathbf{x}-\boldsymbol{\mu})^T \boldsymbol{\Sigma}^{-1} (\mathbf{x}-\boldsymbol{\mu})} \quad (2)$$

Under the assumption of a multivariate normal distribution of the spectral scores, the confidence boundary is established using Hotelling's

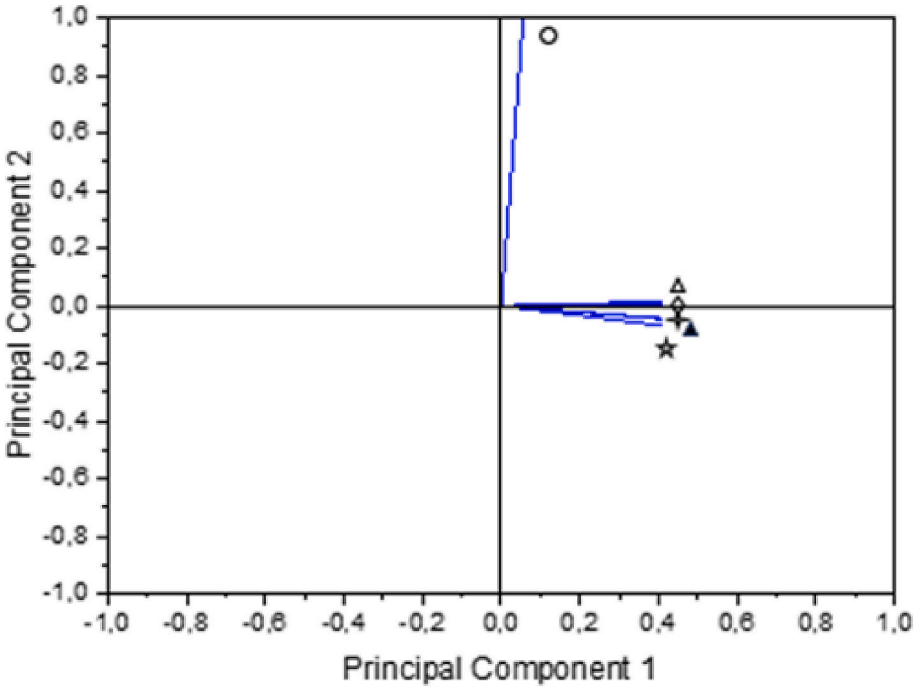

Fig. 6. Multiplication coefficients for red pigments. Multiplication coefficients to be used to obtain the red Raman spectra of the respective samples. (For interpretation of the references to color in this figure legend, the reader is referred to the web version of this article.)

T^2 statistic, which is related to the *F*-distribution:

$$T^2 = n(\mathbf{x} - \bar{\mathbf{x}})^T \mathbf{\Sigma}^{-1} (\mathbf{x} - \bar{\mathbf{x}}) \leq \frac{p(n-1)}{n-p} F_\alpha(p, n-p) \quad (3)$$

where n is the number of baseline samples in the reference manuscript class, p is the number of included principal components (here, $p = 2$), and α is the significance level (typically set at 0.05 for a 95% confidence interval).

In the specific case of the Bolognese 14th-century reference class discussed below, $n = 2$ independent manuscripts and $p = 2$ principal components are used; the rank of the sample covariance matrix is therefore at most $n - 1 = 1$, the matrix is singular and cannot be inverted, and $n - p = 0$ in the equation above, so that the corresponding critical value of the F-distribution, and hence the 95% confidence ellipse, is mathematically undefined and shown in Fig. 7 as a descriptive PC1–PC2 score plot. In principle, such a region could define the boundaries of a "material-profile compatibility region" for a specific scriptorium or historical batch, although, as noted above, it cannot currently be computed as a valid statistical confidence region for the present dataset. In a SIMCA framework, a localized PCA model is built for each manuscript class independently; an unclassified or newly analyzed sample is projected onto each model, and it is either accepted within the 95% confidence ellipse or flagged as an outlier, this is the general SIMCA principle described in the literature. As clarified above and in Section 3.5 and Section 3.6, a sample falling outside a reference region indicates only incompatibility with that reference group and cannot by itself be interpreted as evidence of forgery, restoration, or incorrect provenance. Alternatively, the LDA approach calculates sharp linear decision boundaries that maximize between-class variance while minimizing within-class variance, providing a posterior probability of assignment for the query sample.

It should be emphasized that this approach is based on the spectral response of pigments, inks, and support materials, not on direct geographical or historical information; provenance labels are used only to interpret the resulting spectral groupings. The differences observed between manuscripts may simultaneously reflect several concurrent factors, including the specific ink chemistry used (e.g., carbon black vs. iron-gall ink), differences in support material (paper vs. parchment), the date of production, the conservation history and any past restoration, and the specific formulation of the pigments/inks employed. The present results therefore show, at most, that the material-spectral profile of Tratado de Matematicas is incompatible with that of the two Clementina reference examples; they do not demonstrate that a generalizable "14th-century Bolognese provenance signal" has been identified. A sample falling outside the reference region indicates only incompatibility with that specific reference material-profile group; it cannot, by itself, be interpreted as evidence of incorrect provenance, later restoration, or forgery.

As a practical demonstration of this preliminary approach, the classification models were tested, for illustrative purposes only, using the Raman PCA1–PC2 coordinates extracted from our black and yellow pigment datasets (Tables S3 and S4); the multiblock data-fusion strategy described in Section 3.6 was not applied to this demonstration. Table 6 reports the obtained geometric comparison while Fig. 7 provides a descriptive PC1–PC2 score plot for black inks.

The two 14th-century Bolognese legal manuscripts (Clementine by

Table 6
Descriptive comparison of black and yellow reference examples and comparison sample in PCA space.

Dataset	Reference examples	Comparison sample	Relative position in PCA space
Black	Clementine (Giovanni da Legnano); Clementine (Giovanni Calderini)	Tratado de Matematicas	Clearly separated from the reference examples along PC2 (PC2 ≈ 0.86 vs. ≈ 0.00 / −0.38 for the reference examples)
Yellow	Biblicae Historiae*; Clementine (Giovanni da Legnano)	Tratado de Matematicas	Clearly separated from the reference examples along PC2

* Unlike the Black dataset, no second 14th-century Bolognese manuscript with a genuine (non-gold) yellow pigment was available: Adiciones Johannis Calderini shows saturation due to gold rather than a yellow pigment (Table 2). Biblicae Historiae is therefore included here only as a second illustrative point sharing the PCA space, not as a chronologically consistent member of the 14th-century Bolognese reference cohort; this pairing should not be read as a validated "Bolognese yellow" reference class.

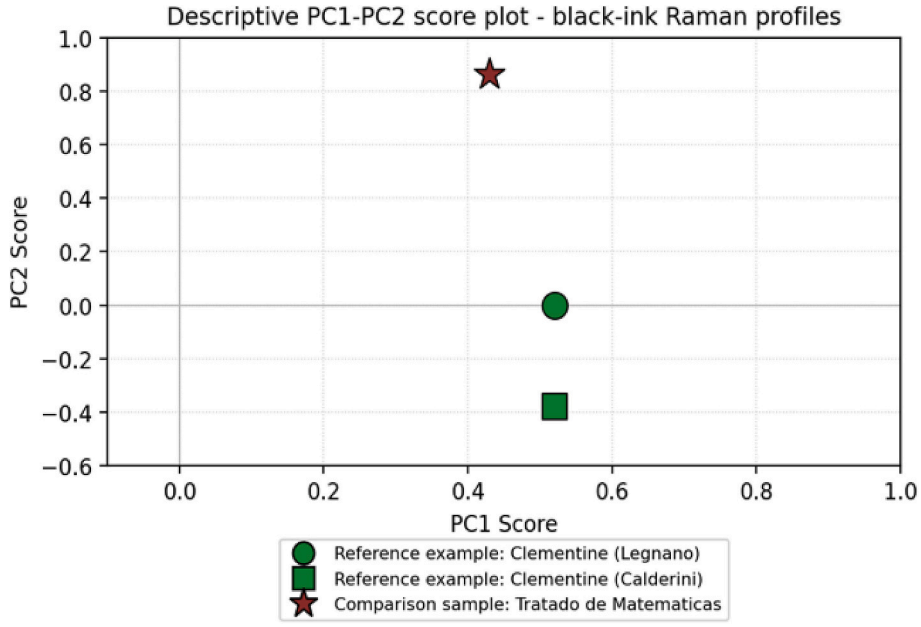

Fig. 7. Descriptive PC1–PC2 score plot of the measured black-ink Raman profiles. The two Clementina texts are shown as reference examples of the 14th-century Bolognese group; Tratado de Matematicas is shown as a comparison sample. The plot illustrates the geometric separation of the measured black-ink profiles in the selected PCA space.

Giovanni da Legnano and Adiciones Johannis Calderini) form a tight cluster in the PC1–PC2 plane. Tratado de Matematicas (characterized by a distinctly different PC2 score of 0.86175, Table S3), used here as a comparison sample, falls clearly outside this cluster. Given $n = 2$, this separation can only be described geometrically; it does not support a statistically valid outlier test or classification probability (see discussion above).

It should further be noted that the Joannes de Lignano and Johannis Calderini manuscripts, having been used to define the Bolognese 14th-century reference cohort, are also the reference examples listed in Table 6; any resemblance reported for them therefore reflects the reclassification of training data against their own reference class rather than an independent prediction.

The same caution applies to the Yellow dataset. Because Adiciones Johannis Calderini does not contain a genuine yellow pigment (Table 2), Biblicae Historiae was used as the second point defining the Yellow dataset shown in Table 6, even though it does not belong to the 14th-century Bolognese cohort (Section 2.1). Consequently, the Yellow row in Table 6 should be read as a simple two-point geometric comparison in PCA space, not as evidence of compatibility with a chronologically coherent Bolognese reference group.

The present study does not include independent manuscript-level training, validation, and test sets. The identity, production date, and documented provenance of Tratado de Matematicas are already known (Section 2.1); it therefore functions only as a comparison sample used to simulate the query procedure, and should not be described as a genuinely unknown manuscript.

Given the very limited number of independent manuscripts available ($n = 2$ for the Bolognese reference material-profile group and $n = 1$ for the comparison sample), the SIMCA and LDA analyses presented in this section are intended as an illustrative, exploratory proof of concept rather than as formally validated statistical classifiers. With such small sample sizes, quantities such as covariance estimates, prior probabilities, and posterior classification probabilities cannot be reliably estimated. The relative positions shown in Fig. 7 illustrate, at a conceptual level, the separation observed among the analyzed samples on the basis of their PC1/PC2 coordinates. Since this separation may also partly reflect differences in support (paper vs. parchment) and ink chemistry (iron-gall ink vs. carbon black) rather than provenance alone, these results should not be interpreted as a validated tool for authenticity verification or provenance identification at this stage. A larger set of independent manuscripts per class would be needed to disentangle a genuine provenance signal from these confounding material factors.

3.6. *Future work: a proposed multiblock data-fusion strategy*

The classification results reported above (Table 6, Fig. 7) are based solely on the Raman PCA1–PC2 coordinates of the black and yellow datasets (Tables S3, S4); the multiblock data-fusion strategy outlined below was not implemented in the present demonstration and is proposed here as a direction for future, larger-scale studies.

A critical challenge in consolidating diverse spectral inputs into a unified classification model lies in the integration of colorimetric Lab coordinates. As demonstrated in our photoluminescence analysis (Section 3.2), several pigments, particularly the red and blue inks across the Explicit Biblia and Compendium, exhibit significant luminescence contributions when excited. This secondary emission introduces a predictable artifact in the Fiber Optic Reflectance Spectroscopy (FORS) profiles, artificially altering the reflectance curves and, consequently, distorting the calculated Lab coordinates. Including compromised Lab data would inject systematic error into any future distance-based calculation, leading to severely skewed confidence regions.

To address this physical interference, a bifurcated Data Fusion strategy could be adopted depending on the photophysical matrix of the sample. For luminescent pigments/areas, the classification model would bypass the colorimetric coordinates entirely; instead, a low-level data fusion matrix could be constructed by concatenating the normalized Raman spectral vectors, the luminescence-corrected (baseline-subtracted) FORS reflectance profiles, and the deconvoluted photoluminescence emission bands (such as the binder/support emission peaks isolated between 630 and 660 nm). The baseline-subtracted, rather than the raw, reflectance profile is used in this block because the raw profile remains affected by the same luminescence artifact described in Section 3.2; pairing it directly with the deconvolved emission bands would count the underlying emission contribution twice, inflating its apparent weight in any future distance-based or discriminant model. For non-luminescent pigments/areas, where no luminescent artifact distorts the reflectance, dimensionality could instead be optimized by combining the molecular fingerprint of the Raman spectra, the electronic transitions from FORS, and the macrochromatic Lab coordinates.

4. Conclusions

Raman spectroscopy, reflectivity, and luminescence techniques were used for the characterization of miniatures present in some manuscripts from the 14th to the 17th centuries, preserved at the University Library of Cagliari. Raman spectroscopy allowed the identification of the pigments used and the type of support. The results obtained were consistent with the materials historically employed. The identified supports were paper and parchment, both commonly used in the medieval and early modern periods. The pigments recognized, cinnabar, malachite, azurite, purpurin, and orpiment, are natural mineral colors that were typical in medieval manuscripts.

Principal Component Analysis (PCA) was also applied to the collected data. The PCA results demonstrated the effectiveness of this technique highlighting principal components that predominantly reflect the spectral features associated with individual pigment components present in the materials, and in comparing pigment compositions, achieving satisfactory data clustering. However, in the specific case under consideration, this technique may prove less effective if the number of available samples is not sufficient for a satisfactory PCA. Since experimental points revealed more than two components per color, the use of a greater number of principal components would be preferable if a significantly larger sample set were available. On the other hand, with only a few samples, as in the case of this study, doing so would undermine the effectiveness of PCA as a tool for data aggregation.

Beyond exploratory PCA, supervised chemometric approaches based on SIMCA and LDA were investigated as preliminary, illustrative proof of concept for future provenance assessment and manuscript classification. In this exploratory analysis, the Raman spectroscopic dataset showed a clear geometric separation for the small number of manuscripts examined, which differ in both historical origin and material composition; as detailed in Section 3.4, the colors used for this demonstration (black and yellow) were themselves selected post hoc because they showed the largest separation, so this outcome should be treated as hypothesis-generating rather than as a measure of achievable classification accuracy. Given the very limited number of independent manuscripts available, these results should be regarded as a preliminary, proof-of-concept illustration of the potential of chemometric methodologies for cultural heritage diagnostics, rather than as validated evidence for authenticity verification.

Colorimetric characterization provided spectra compatible with those expected for the considered pigment types. However, in some cases, the reflectance measurement showed a background, likely due to the presence of some binder or originated from the luminescence of the writing support (paper or parchment).

Luminescence measurements revealed emission bands at positions different from those expected for the identified pigments in nearly all samples. In all cases, the peak position was between 630 and 660 nm, which can be attributed to the binders used.

The validity and effectiveness, as well as some limitations, of the

techniques used for the analysis of materials in the field of cultural heritage, were demonstrated in the present case for miniatures of valuable ancient texts. Specifically, for near-IR Raman spectroscopy, the difficulties due to the low power employed did not prevent the collection of a usable spectrum, except for a few sporadic cases.

Analysis of the obtained spectra allowed the identification of the main compounds and the detection of impurities responsible for peak shifts. FORS measurements confirmed the reflectance spectra of the individual compounds; however, excitation with a white lamp caused the luminescence contribution of some additional elements present in the samples or in the writing support. Using photoluminescence techniques, this emission was studied to determine its origin and possible assignment.

Results indicate that the pigments used for the text and for the miniatures were consistent. This observation suggests that the same batches of pigments were likely employed for both writing and illustrating, reflecting an integrated workflow or a shared palette within the scriptorium [23,24].

To the best of our knowledge, no previous studies have simultaneously applied Raman spectroscopy, reflectance measurement, luminescence analysis and PCA for the characterization of miniatures. While these techniques have been employed in various combinations, their integration into a single non-invasive analysis is uncommon. The present results confirm the complementarity of Raman spectroscopy, FORS, luminescence spectroscopy, and colorimetric analysis for the non-invasive characterization of historical manuscripts. Furthermore, the complementary use of these analytical techniques, together with exploratory Raman-based chemometric analysis, enhances the interpretative potential of the material characterization. The preliminary SIMCA and LDA models illustrate, in a preliminary and exploratory manner, how combined spectroscopic information might in future be used, after appropriate validation on independent manuscript collections, to support provenance-related screening. Although the limited number of available manuscripts prevents the construction of fully generalized predictive models, the proposed workflow represents a promising foundation for future large-scale studies aimed at developing robust automated tools for manuscript attribution, conservation support, and anti-counterfeiting applications, provided that independent, adequately sized manuscript collections become available (see Section 3.5).

CRediT authorship contribution statement

Stefania Porcu: Writing – review & editing, Writing – original draft, Visualization, Supervision, Project administration, Methodology, Investigation, Conceptualization, Data curation, Formal Analysis. **Giulia Pruna:** Writing – original draft, Methodology, Data curation. **Lorenzo Minnai:** Writing – original draft, Methodology, Data curation. **Giancarlo Cappellini:** Visualization, Methodology, Conceptualization. **Daniele Chiriu:** Writing – review & editing, Writing – original draft, Visualization, Supervision, Project administration, Methodology, Investigation, Conceptualization, Formal Analysis, Funding acquisition.

Declaration of competing interest

The authors declare that they have no known competing financial interests or personal relationships that could have appeared to influence the work reported in this paper.

Acknowledgements

All the authors acknowledge the University Library of Cagliari (BUCA).

Giancarlo Cappellini acknowledges COST Action CA21126– Carbon molecular nanostructures in space (NanoSpace), supported by COST (European Cooperation in Science and Technol ogy)– EU; Project AISAC-PNRR by the Italian Government (Ministero delle Imprese e del Made in Italy-MIMIT), Fondo per la Crescita Sostenibile– Accordi per l'innovazione di cui al D.M. 31 dicembre 2021 e D.D. 18 marzo 2022, grant no. F/310035/05/X56; partial financial support from IDEA-AISBL Bruxelles.

Funding

This research was funded by Fondazione di Sardegna, project FDS2022 "New diagnostic techniques for ancient books restauration and conservation" CUP F73C23001560007.

Appendix A. Supplementary data

Supplementary data to this article can be found online at https://doi.org/10.1016/j.saa.2026.128783.

Data availability

Data will be made available on request.

References

[1] X. Zabulis, N. Partarakis, E. Zidianakis, D. Kaplanidi, A critical review of the function of intangible cultural heritage as a driver for social resilience and cohesion, Encyclopedia 5 (2025) 1–37, https://doi.org/10.3390/encyclopedia5040189.
[2] M.R. Reshma, B. Kannan, V.P. Jagathy Raj, S. Shailesh, Cultural heritage preservation through dance digitization: a review, Digital Appl. Archaeol. Cult. Herit. 28 (2023) e00257, https://doi.org/10.1016/j.daach.2023.e00257.
[3] M. Vecco, A definition of cultural heritage: from the tangible to the intangible, J. Cult. Herit. 11 (2010) 321–324, https://doi.org/10.1016/j.culher.2010.01.006.
[4] M. Odlyha, Introduction to the preservation of cultural heritage, J. Therm. Anal. Calorim. 104 (2011) 399–403, https://doi.org/10.1007/s10973-011-1421-0.
[5] R.G. Castor, A systematic review of cultural memory and heritage management : Global perspectives and integrated analysis, 2026, pp. 1–21.
[6] C. Holtorf, The changing contribution of cultural heritage to society, Mus. Int. 63 (2011) 8–16, https://doi.org/10.1111/j.1468-0033.2012.01758.x.
[7] K. Ounanian, J.P.M. van Tatenhove, C.J. Hansen, A.E. Delaney, H. Bohnstedt, E. Azzopardi, W. Flannery, H. Toonen, J.O. Kenter, L. Ferguson, M. Kraan, J. V. Macias, M. Lamers, C. Pita, A.M. Ferreira da Silva, H. Albuquerque, F.L. Alves, D. Mylona, K. Frangoudes, Conceptualizing coastal and maritime cultural heritage through communities of meaning and participation, Ocean Coast. Manag. 212 (2021), https://doi.org/10.1016/j.ocecoaman.2021.105806.
[8] I. Online, Int. J. Humanit. Soc. Sci. 10 (2025) 1–7. The role of cultural heritage in shaping national identity : Abstract.
[9] H. Li, K. Ikebe, T. Kinoshita, J. Chen, D. Su, J. Xie, How heritage promotes social cohesion: an urban survey from Nara city, Japan, Cities 149 (2024) 104985, https://doi.org/10.1016/j.cities.2024.104985.
[10] D. Cora, Miniature painting in eighteenth-century England: the case of William Pether (1739–1821), Arts 11 (2022) 61, https://doi.org/10.3390/arts11030061.
[11] P. Singh Dr., Miniature paintings: Riches & Legacy of Indian cultural heritage, Educ. Admin. Theory Pract. 30 (2024) 13606–13622, https://doi.org/10.53555/kuey.v30i5.5898.
[12] K. Leonhard, Painted gems. The color worlds of portrait miniature painting in sixteenth- and seventeenth-century Britain, Early Sci. Med. 20 (2015) 428–457, https://doi.org/10.1163/15733823-02046p06.
[13] M. Shahi, R. Rajabi, F. Masoumzadeh, CNN-based classification of Persian miniature paintings from five renowned schools, Digital Appl. Archaeol. Cult. Herit. 36 (2025) e00397, https://doi.org/10.1016/j.daach.2024.e00397.
[14] P. Knipe, K. Eremin, M. Walton, A. Babini, G. Rayner, Materials and techniques of Islamic manuscripts, Herit. Sci. 6 (2018) 1–40, https://doi.org/10.1186/s40494-018-0217-y.
[15] E. Priego de los Santos, J. Herraez Boquera, J.L. Denia Rios, J.L. Regidor Ros, Digital reintegration of fragmented wall paintings: 3D texture mapping of historical photographs in the Santos Juanes church restoration, Digit. Appl. Archaeol. Cult. Herit. 40 (2026), https://doi.org/10.1016/j.daach.2026.e00514.
[16] G. Stafford, Between the living and the dead: use, reuse, and imitation of painted portraits in late antiquity, J. Rom. Archaeol. 35 (2022) 683–712, https://doi.org/10.1017/S1047759422000319.
[17] M. Ciatti, C. Frosinini, Structural conservation of panel paintings at the Opificio delle Pietre dure in florence: method, theory, and practice, 2016.
[18] Rijks Museum, The conservation of panel paintings and related objects, 2014, pp. 1–226.
[19] W. Zhang, S. Wang, H. Guo, Study on the aging effects of relative humidity on the primary chemical components of palm leaf manuscripts, Polymers 17 (2025), https://doi.org/10.3390/polym17010083.

[20] A. Amat, C. Miliani, B.G. Brunetti, Non-invasive multi-technique investigation of artworks: a new tool for on-the-spot data documentation and analysis, J. Cult. Herit. 14 (2013) 23–30, https://doi.org/10.1016/j.culher.2012.02.015.
[21] S. Lyu, X. Yang, N. Pan, M. Hou, W. Wu, M. Peng, X. Zhao, Spectral heat aging model to estimate the age of seals on painting and calligraphy, J. Cult. Herit. 46 (2020) 119–130, https://doi.org/10.1016/j.culher.2020.08.005.
[22] A. Tonazzini, E. Salerno, Z.A. Abdel-Salam, M.A. Harith, L. Marras, A. Botto, B. Campanella, S. Legnaioli, S. Pagnotta, F. Poggialini, V. Palleschi, Analytical and mathematical methods for revealing hidden details in ancient manuscripts and paintings: a review, J. Adv. Res. 17 (2019) 31–42, https://doi.org/10.1016/j.jare.2019.01.003.
[23] X. Zhang, Y. Yan, J. Yao, S. Jin, Y. Tang, Chemistry directs the conservation of paper cultural relics, Polym. Degrad. Stab. 207 (2023) 110228, https://doi.org/10.1016/j.polymdegradstab. 2022.110228.
[24] W. Zhang, S. Wang, H. Guo, Effects of environmental factors on the mechanical properties of palm leaf manuscripts: natural aging, temperature, relative humidity, and light radiation, Polymers (Basel) 17 (2025) 1–18, https://doi.org/10.3390/polym17233229.
[25] X. Ye, Y. Chen, L. Peng, X. Yang, Y. Bai, Application of spectroscopy technique in cultural heritage: systematic review and bibliometric analysis, Npj Heritage Sci. 13 (2025) 1–19, https://doi.org/10.1038/s40494-025-01622-0.
[26] D. Chiriu, F.A. Pisu, P.C. Ricci, C.M. Carbonaro, Application of raman spectroscopy to ancient materials: models and results from archaeometric analyses, Materials 13 (2020), https://doi.org/10.3390/MA13112456.
[27] I.A. Balakhnina, N.N. Brandt, A.Y. Chikishev, N.L. Rebrikova, Raman microspectroscopy of old paper samples with foxing, Appl. Spectrosc. 68 (2014) 495–501, https://doi.org/10.1366/13-07222.
[28] T.C. David, F.A. Pisu, S. Porcu, C.M. Carbonaro, J. Kodric, D. Chiriu, Effects of saline solutions on paper-based cultural heritage: non-invasive techniques for studying flooded ancient books, Heritage 8 (2025) 40, https://doi.org/10.3390/heritage8020040.
[29] V. Pinna, S. Porcu, G. Siotto, E. Tuveri, P.C. Ricci, E. Lodo, P. Coli, R. Cardia, D. Chiriu, Development of comparative and machine learning–based methodologies for the identification of inks applicable in the field of cultural heritage and forensic science, Talanta 305 (2026) 129678, https://doi.org/10.1016/j.talanta.2026.129678.
[30] D. Chiriu, P.C. Ricci, G. Cappellini, Raman characterization of XIV–XVI centuries Sardinian documents: inks, papers and parchments, Vib. Spectrosc. 92 (2017) 70–81, https://doi.org/10.1016/j.vibspec.2017.05.007.
[31] L. Pronti, M. Romani, L. Lanteri, F. Bizzarri, C. Colantonio, C. Pelosi, C. Ruberto, L. Castelli, A. Mazzinghi, V. Spizzichino, M. Cestelli Guidi, Non-invasive investigation of a 16th-century illuminated scroll: pigments, fillers, and metal-based decorations, Minerals 15 (2025) 1–24, https://doi.org/10.3390/min15121252.
[32] M. Aceto, E. Calà, Analytical evidences of the use of iron-gall ink as a pigment on miniature paintings, Spectrochim. Acta A Mol. Biomol. Spectrosc. 187 (2017) 1–8, https://doi.org/10.1016/j.saa.2017.06.017.
[33] P. Ricciardi, A. Pallipurath, The five colours of art: non-invasive analysis of pigments in Tibetan prints and manuscripts, brill's Tibetan studies, Library 39 (2016) 485–500, https://doi.org/10.1163/9789004316256_023.
[34] I. Nastova, O. Grupče, B. Minčeva-Šukarova, M. Ozcatal, L. Mojsoska, Spectroscopic analysis of pigments and inks in manuscripts: I. Byzantine and post-byzantine manuscripts (10-18th century), Vib. Spectrosc. 68 (2013) 11–19, https://doi.org/10.1016/j.vibspec.2013.05.006.
[35] F.A. Pisu, C.M. Carbonaro, P.C. Ricci, S. Porcu, D. Chiriu, Cadmium yellow pigments in oil paintings: optical degradation studies utilizing 3D fluorescence mapping supported by Raman spectroscopy and colorimetry, Heritage 7 (2024) 2426–2443, https://doi.org/10.3390/heritage7050115.
[36] B. Capone, P. Biocca, P. Corsi, C. Meneghini, M. Bicchieri, Does the Artemidorus papyrus have multiple lives? Seeking for the answer in the inks through a Raman and PCA analysis, J. Cult. Herit. 48 (2021) 1–10, https://doi.org/10.1016/j.culher.2021.02.003.
[37] A. Coccato, M.C. Caggiani, An overview of principal components analysis approaches in Raman studies of cultural heritage materials, J. Raman Spectrosc. 55 (2024) 125–147, https://doi.org/10.1002/jrs.6621.
[38] B. Yogurtcu, N. Cebi, A.T. Koçer, A. Erarslan, A review of non-destructive Raman spectroscopy and chemometric techniques in the analysis of cultural heritage, Molecules 29 (2024), https://doi.org/10.3390/molecules29225324.
[39] J. Riu, B. Giussani, Analytical chemistry meets art: the transformative role of chemometrics in cultural heritage preservation, Chemom. Intell. Lab. Syst. 247 (2024) 105095, https://doi.org/10.1016/j.chemolab.2024.105095.
[40] C. Grazia, C. Clementi, C. Miliani, A. Romani, Photophysical properties of alizarin and purpurin Al(iii) complexes in solution and in solid state, Photochem. Photobiol. Sci. 10 (2011) 1249–1254, https://doi.org/10.1039/c1pp05039g.
[41] M. Longoni, N. Hopes, F. Rossi, M.R. Tessera, M. Petoletti, S. Bruni, Inside the scriptorium: non-invasive in situ identification of dyes in illuminated manuscripts by microspectrofluorimetry and multivariate analysis: the Crescenzago choir books (end 15th century) as a case study, Heritage 6 (2023) 2006–2019, https://doi.org/10.3390/heritage6020108.